Error Performance Analysis of Coded Wireless Optical Links over Atmospheric Turbulence Channels

Murat Uysal
Department of Electrical and Computer Engineering
University of Waterloo, Waterloo, ON, Canada, N2G3L1
muysal@ece.uwaterloo.ca

Jing (Tiffany) Li
Department of Electrical and Computer Engineering
Lehigh University, Bethlehem, PA, USA 18015
jingli@eecs.lehigh.edu

***Abstract*—We analyze the error rate performance of coded wireless optical links operating over atmospheric channels, where the turbulence-induced fading is modeled by the negative exponential distribution, K distribution and I-K distribution. First, we derive bounds on the pairwise error probability (PEP) for each fading model and then apply the transfer function technique in conjunction with derived PEP bounds to obtain bit error rate performance. Simulation results are also included to confirm the analytical results.**

***Keywords*—Atmospheric turbulence channel, free-space optical communication, pairwise error probability, error performance analysis.**

I. INTRODUCTION

Wireless optical communications, also known as free-space optical (FSO) communications, is a cost-effective and high bandwidth access technique and is receiving growing attention with recent commercialization successes [1]. In a wireless optical communication system, optical transceivers communicate directly through the air to form point-to-point line-of-sight links. One major impairment over FSO links is the atmospheric turbulence, which occurs as a result of the variations in refractive index due to inhomogeneties in temperature and pressure fluctuations. The atmospheric turbulence causes fluctuations at the received signal (i.e., intensity fading, also known as scintillation in optical communication terminology [2]), severely degrading the link performance. Error control coding as well as diversity techniques can be used over FSO links to improve the error rate performance [3, 4]. In [4], Zhu and Kahn derived an approximate upper bound on the pairwise error probability of a coded wireless optical communication system over turbulence channels assuming lognormal channel model and provided upper bounds on the bit error rate performance using transfer function technique. Although lognormal distribution is the most widely used model for the probability density function (pdf) of the irradiance due to its simplicity, this pdf model is only applicable to weak turbulence regime. Due to the limitations of lognormal model, many statistical models have been proposed over the years to describe atmospheric turbulence channels under a wide range of turbulence conditions [2]. Among the various theoretical models, we focus on three pdfs, namely *negative exponential distribution*, *K distribution* and *I-K distribution*. While the first two models are used to describe strong turbulence conditions, *I-K* distribution which is essentially an extension of *K* distribution covers also weak fluctuation regimes. In this paper, we will derive error performance bounds for coded wireless optical links operating over atmospheric channels, where the turbulence-induced fading is described by the aforementioned channel models.

II. DISTRIBUTION MODELS FOR TURBULENCE-INDUCED INTENSITY FADING

In this section, we review each of the three channel models used throughout the paper and discuss their relations among them.

II. a. *Negative exponential channel*

Most of the theoretical distributions proposed for the intensity fluctuations of an electromagnetic wave propagating through atmospheric turbulence are based on mathematical models which relate discreet scattering regions in the turbulent medium to the individual inhomogeneties in the electromagnetic wave. If the number of discrete scattering regions is sufficiently large, the radiation field of the electromagnetic wave is approximately Gaussian and therefore the irradiance statistics of the field are governed by the negative exponential distribution, given as [2]

$$f(I) = \exp(-I),\ I > 0 \tag{1}$$

This distribution model assumes very large number of scatterers and can be considered as a limiting case.

II. b. *K channel*

One of the widely accepted models under strong turbulence regime is the *K* distribution. This distribution was originally proposed to model non-Rayleigh sea echo [5], but it was later discovered that it provides excellent agreement with experimental data in a variety of experiments involving radiation scattered by strong turbulent media [6, 7]. The *K* distribution can be derived from a modulation process wherein the conditional pdf of irradiance is governed by the negative exponential distribution with mean irradiance following the gamma distribution. The resulting distribution is given as [2]

$$f(I)=\frac{2}{\Gamma(\alpha)}\alpha^{(\alpha+1)/2}I^{(\alpha-1)/2}K_{\alpha-1}\left(2\sqrt{\alpha I}\right),\ I>0, \tag{2}$$

where α is a positive parameter related to the effective number of scatterers. Here $\Gamma(.)$ and $K_a(.)$ stand for the gamma function and the modified Bessel function of the second kind of order *a*, respectively. In the limiting case of $\alpha\to\infty$, the *K* distribution reduces to the negative exponential distribution.

II. c. *I-K* channel

The *K* channel is applicable under only strong turbulence conditions. In [8], it is discussed that the coherent addition of a constant amplitude component and *K* distributed noise can lead to a model which will also cover the weak turbulence regime. However, this so-called *homodyned K* (*H-K*) distribution does not lend itself to an easily tractable analytical form, limiting its usefulness. The *I-K* distribution [9] was developed as an approximation to the *H-K* distribution. Both models demonstrate comparable statistics, however the *I-K* distribution has the advantage of computational simplicity, providing a closed-form expression for its pdf. The *I-K* pdf is given by [9]

$$f(I)=\begin{cases}2\alpha(1+\rho)\left(1+\dfrac{1}{\rho}\right)^{\frac{\alpha-1}{2}}I^{\frac{\alpha-1}{2}}K_{\alpha-1}\left(2\sqrt{\alpha\rho}\right)I_{\alpha-1}\left(2\sqrt{\alpha(1+\rho)I}\right), \\ 0<I<\rho/(1+\rho)\end{cases} \tag{3}$$

$$\begin{cases}2\alpha(1+\rho)\left(1+\dfrac{1}{\rho}\right)^{\frac{\alpha-1}{2}}I^{\frac{\alpha-1}{2}}I_{\alpha-1}\left(2\sqrt{\alpha\rho}\right)K_{\alpha-1}\left(2\sqrt{\alpha(1+\rho)I}\right), \\ I>\rho/(1+\rho)\end{cases}$$

where $I_a(.)$ is the modified Bessel function of first kind of order *a* and ρ is the coherence parameter defined as the ratio of power in the coherent component to that in scattered components. As ρ goes to zero (i.e. no coherent component), the *I-K* distribution reduces to the *K* distribution.

III. Derivation Of PEP

The PEP represents the probability of choosing the coded sequence $\hat{\boldsymbol{X}}=(\hat{x}_1,...,\hat{x}_N)$ when indeed $\boldsymbol{X}=(x_1,...,x_N)$ was transmitted. Here, we consider intensity modulation and direct detection (IM/DD) links using on-off keying (OOK). Following [4], we assume that the noise can be modeled as additive white Gaussian noise (AWGN) with zero mean and variance $N_0/2$, independent of the on/off state of the received bit. Furthermore, we assume that the turbulence-induced fading remains constant over one bit interval and changes from one interval to another in an independent manner. Under the assumption of maximum likelihood soft decoding and perfect channel state information, the conditional PEP with respect to intensity fading coefficients $\boldsymbol{I}=(I_1,I_2,...,I_N)$ is given as [4]

$$P\left(\boldsymbol{X},\hat{\boldsymbol{X}}\middle|\boldsymbol{I}\right)=Q\left(\sqrt{\frac{E_s}{2N_0}\sum_{k\in\Omega}I_k^2}\right) \tag{4}$$

where E_s is the total transmitted energy (without turbulence effects) and Ω is the set of bit intervals' locations where $\boldsymbol{X}$ and $\hat{\boldsymbol{X}}$ differ from each other. Defining the signal-to-noise ratio as $\tau=E_s/N_0$ and using the upper bound on Gaussian-*Q* function, i.e. $Q\left(\sqrt{z}\right)\le 0.5\exp(-z/2)$, we obtain

$$P\left(\boldsymbol{X},\hat{\boldsymbol{X}}\middle|\boldsymbol{I}\right)\le\frac{1}{2}\exp\left(-\frac{\tau}{4}\sum_{k\in\Omega}I_k^2\right)=\frac{1}{2}\prod_{k\in\Omega}\exp\left(-\frac{\tau}{4}I_k^2\right). \tag{5}$$

To obtain unconditional PEP, we need to take an expectation of (5) with respect to I_k. Under the assumption of symbol-by-symbol interleaving which guarantees independency among I_k, we obtain

$$P\left(\boldsymbol{X},\hat{\boldsymbol{X}}\right)\le\frac{1}{2}\left[\int_0^\infty\exp\left(-\frac{\tau}{4}I^2\right)f(I)dI\right]^{|\Omega|} \tag{6}$$

where $f(I)$ represents the pdf of the turbulence-induced intensity fading and $|\Omega|$ is the cardinality of Ω and corresponds to the length of the error event.

III. a. *PEP over the negative exponential channel*

Substituting pdf expression for the negative exponential channel given by (1) in (6) and using the closed form solution for the resulting integral from [10, p.113, Eq.2.33], we obtain

$$P\left(\boldsymbol{X},\hat{\boldsymbol{X}}\right)\le\frac{1}{2}\left[\sqrt{\frac{4\pi}{\tau}}\exp\left(\frac{1}{\tau}\right)Q\left(\sqrt{\frac{2}{\tau}}\right)\right]^{|\Omega|}. \tag{7}$$

III. b. *PEP over the K channel*

Substituting pdf expression for the *K* channel given by (2) in (6), we have

$$P\left(\boldsymbol{X},\hat{\boldsymbol{X}}\right)\le\frac{1}{2}\left[\frac{2\alpha^{(\alpha+1)/2}}{\Gamma(\alpha)}\int_0^\infty\exp\left(-\frac{\tau}{4}I^2\right)I^{\frac{\alpha-1}{2}}K_{\alpha-1}\left(2\sqrt{\alpha I}\right)dI\right]^{|\Omega|} \tag{8}$$

which, unfortunately, does not have a closed form solution. In the following, we will derive an approximate bound based on the series representation of the modified Bessel function, which is given as [10, p.971, eq. 8.446]

$$K_a(z)=\frac{1}{2}\sum_{k=0}^{a-1}(-1)^k\frac{(a-k-1)!}{k!}\left(\frac{z}{2}\right)^{-(a-2k)} \tag{9}$$

$$+(-1)^{a+1}\sum_{k=0}^{\infty}\frac{1}{k!(n+k)!}\left(\frac{z}{2}\right)^{a+2k}\left[\ln\frac{z}{2}-\frac{1}{2}\psi(k+1)-\frac{1}{2}\psi(a+k+1)\right]$$

where $\psi(.)$ is the Euler's psi function. Substituting (9) in (8) and after some mathematical manipulation, (9) can be expressed in a summation form as

$$P\left(\boldsymbol{X},\hat{\boldsymbol{X}}\right)\le\frac{1}{2}\left[\frac{2\alpha^{(\alpha+1)/2}}{\Gamma(\alpha)}\right]^{|\Omega|}\left[\sum_{k=0}^{\alpha-2}a_k\int_0^\infty\exp\left(-\frac{\tau}{4}I^2\right)I^k dI\right.$$

$$+\sum_{k=0}^{\infty}b_k\int_0^\infty\exp\left(-\frac{\tau}{4}I^2\right)I^{\alpha+k-1}\ln\left(\sqrt{\alpha I}\right)dI \tag{10}$$

$$\left.+\sum_{k=0}^{\infty}c_k\int_0^\infty\exp\left(-\frac{\tau}{4}I^2\right)I^{\alpha+k-1}dI\right]^{|\Omega|}$$

where a_k, b_k and c_k are defined as

$$a_k = \frac{(-1)^k}{2}\frac{(\alpha-k-2)!}{k!}\alpha^{-\frac{(\alpha-2k-1)}{2}}, b_k = \frac{(-1)^\alpha}{k!(\alpha+k-1)!}\alpha^{\frac{(\alpha+2k-1)}{2}},$$

$$c_k = \frac{1}{2}\frac{(-1)^{\alpha-1}}{k!(\alpha+k-1)!}\alpha^{\frac{(\alpha+2k-1)}{2}}\left[\psi(k+1)+\psi(k+\alpha)\right].$$

Using $\ln x \approx x-1$, an approximation of (10) can be obtained as

$$P(\boldsymbol{X},\hat{\boldsymbol{X}}) \le \frac{1}{2}\left[\frac{2\alpha^{(\alpha+1)/2}}{\Gamma(\alpha)}\right]^{|\Omega|}\left[\sum_{k=0}^{\alpha-2}a_k\int_0^\infty \exp\left(-\frac{\tau}{4}I^2\right)I^k dI + \sqrt{\alpha}\sum_{k=0}^{\infty}b_k\int_0^\infty \exp\left(-\frac{\tau}{4}I^2\right)I^{\alpha+k-\frac{1}{2}}dI + \sum_{k=0}^{\infty}(c_k-b_k)\int_0^\infty \exp\left(-\frac{\tau}{4}I^2\right)I^{\alpha+k-1}dI\right]^{|\Omega|} \quad (11)$$

The above integrals can be easily solved with the help of [10, p. 364, eq. 3.381.4], yielding the final form for PEP as

$$P(\boldsymbol{X},\hat{\boldsymbol{X}}) \le \frac{1}{2}\left[\frac{\alpha^{(\alpha+1)/2}}{\Gamma(\alpha)}\right]^{|\Omega|}\left[\sum_{k=0}^{\alpha-2}a_k\Gamma\left(\frac{k+1}{2}\right)\left(\frac{\tau}{4}\right)^{-\left(\frac{k+1}{2}\right)} + \sqrt{\alpha}\sum_{k=0}^{\infty}b_k\Gamma\left(\frac{2\alpha+2k+1}{4}\right)\left(\frac{\tau}{4}\right)^{-\left(\frac{2\alpha+2k+1}{4}\right)} + \sum_{k=0}^{\infty}(c_k-b_k)\Gamma\left(\frac{\alpha+k}{2}\right)\left(\frac{\tau}{4}\right)^{-\left(\frac{\alpha+k}{2}\right)}\right]^{|\Omega|}. \quad (12)$$

As it will be demonstrated in the next section, truncating infinite summations in (12) to only a few terms yields a very accurate approximation for all practical α values. It should be also noted that (12) works only for $\alpha \ge 2$ integer values. Since the effective number of discrete scatterers is usually larger than 2, the derived approximate bound is able to provide results for a wide range of practical values.

III. c. *PEP over the I-K channel*

Substituting pdf expression for *I-K* channel given by (3) into (6), we obtain

$$P(\boldsymbol{X},\hat{\boldsymbol{X}}) \le \frac{1}{2}\left[2\alpha(1+\rho)\left(1+\frac{1}{\rho}\right)^{\frac{\alpha-1}{2}}K_{\alpha-1}\left(2\sqrt{\alpha\rho}\right)\times\int_0^{\rho/(1+\rho)}\exp\left(-\frac{\tau}{4}I^2\right)I^{\frac{\alpha-1}{2}}I_{\alpha-1}\left(2\sqrt{\alpha(1+\rho)I}\right)dI + 2\alpha(1+\rho)\left(1+\frac{1}{\rho}\right)^{\frac{\alpha-1}{2}}I_{\alpha-1}\left(2\sqrt{\alpha\rho}\right)\times\int_{\rho/(1+\rho)}^{\infty}\exp\left(-\frac{\tau}{4}I^2\right)I^{\frac{\alpha-1}{2}}K_{\alpha-1}\left(2\sqrt{\alpha(1+\rho)I}\right)dI\right]^{|\Omega|} \quad (13)$$

which does not accept a closed-form solution. As in the previous case, we resort to obtain an approximate upper bound based on the series representation of modified Bessel functions of the first kind $I_a(.)$ and the second kind $K_a(.)$ in (13). For the first integral in (13), replacing $I_a(.)$ by its series representation [10, p.971, eq. 8.445]

$$I_a(z) = \sum_{k=0}^{\infty}\frac{1}{k!\Gamma(a+k+1)}\left(\frac{z}{2}\right)^{a+2k}$$

and using [10, p. 364, eq. 3.381.1] for the resulting integral expression, we have

$$\int_0^{\rho/(1+\rho)}\exp\left(-\frac{\tau}{4}I^2\right)I^{\frac{\alpha-1}{2}}I_{\alpha-1}\left(2\sqrt{\alpha(1+\rho)I}\right)dI = \frac{1}{2}\sum_{k=0}^{\infty}d_k\left(\frac{\tau}{4}\right)^{-\left(\frac{\alpha+k}{2}\right)}\gamma\left(\frac{\alpha+k}{2},\frac{\tau}{4}\left(\frac{\rho}{1+\rho}\right)^2\right) \quad (14)$$

where $d_k = \left[\alpha(1+\rho)\right]^{\frac{\alpha-1+2k}{2}}/k!\Gamma(\alpha+k)$ and $\gamma(.,.)$ stands for the incomplete gamma function defined as in [10, p. 949, eq. 8.350.1]. For the second integral in (13), first we replace $K_a(.)$ by its series representation given by (9) and apply the approximation $\ln\left(\sqrt{\alpha(1+\rho)I}\right) \approx \sqrt{\alpha(1+\rho)I}-1$ in the resulting expression. Then with the help of [10, p. 364, eq. 3.381.3], we write

$$\begin{aligned}&\int_{\rho/(1+\rho)}^{\infty}\exp\left(-\frac{\tau}{4}I^2\right)I^{\frac{\alpha-1}{2}}K_{\alpha-1}\left(2\sqrt{\alpha(1+\rho)I}\right)dI \\ &= \frac{1}{2}\sum_{k=0}^{\alpha-2}e_k\left(\frac{\tau}{4}\right)^{-\left(\frac{k+1}{2}\right)}\Gamma\left(\frac{k+1}{2},\frac{\tau}{4}\left(\frac{\rho}{1+\rho}\right)^2\right) \\ &+ \frac{\sqrt{\alpha(1+\rho)}}{2}\sum_{k=0}^{\infty}f_k\left(\frac{\tau}{4}\right)^{-\left(\frac{2\alpha+2k+1}{4}\right)}\Gamma\left(\frac{2\alpha+2k+1}{4},\frac{\tau}{4}\left(\frac{\rho}{1+\rho}\right)^2\right) \\ &+ \frac{1}{2}\sum_{k=0}^{\infty}(g_k-f_k)\left(\frac{\tau}{4}\right)^{-\left(\frac{\alpha+k}{2}\right)}\Gamma\left(\frac{\alpha+k}{2},\frac{\tau}{4}\left(\frac{\rho}{1+\rho}\right)^2\right)\end{aligned} \quad (15)$$

where $\Gamma(.,.)$ is the incomplete gamma function[1] defined as in [10, p. 949, eq. 8.350.2], where e_k, f_k and g_k are defined as

$$e_k = \frac{(-1)^k}{2}\frac{(\alpha-k-2)!}{k!}\left[\alpha(1+\rho)\right]^{-\frac{(\alpha-2k-1)}{2}},$$

$$f_k = \frac{(-1)^\alpha}{k!(\alpha+k-1)!}\left[\alpha(1+\rho)\right]^{\frac{(\alpha+2k-1)}{2}}$$

$$g_k = \frac{1}{2}\frac{(-1)^{\alpha-1}}{k!(\alpha+k-1)!}\left[\alpha(1+\rho)\right]^{\frac{(\alpha+2k-1)}{2}}\left[\psi(k+1)+\psi(k+\alpha)\right].$$

Substituting (14) and (15) in (13), the final form for PEP is found as in (16). As it will be demonstrated in the next section, truncation of infinite summations in (16) result in a very good approximation. Our numerical results reveal that taking into account only the first four terms in the first summation and the first five terms in the third and fourth summations in (16) yields an accurate approximation for all practical α and ρ values. As in

[1] One should be aware of the different integral periods in $\gamma(.,.)$ and $\Gamma(.,.)$, which are both defined in [10, p.949] as incomplete gamma functions.

the case of derived bound for *K* channel, this bound works for $\alpha \geq 2$ integer values due to the upper limit in the second summation.

$$
\begin{aligned}
P(\boldsymbol{X},\hat{\boldsymbol{X}}) \leq \frac{1}{2}\Bigg[& \alpha(1+\rho)\left(1+\frac{1}{\rho}\right)^{\frac{\alpha-1}{2}} K_{\alpha-1}\left(2\sqrt{\alpha\rho}\right) \\
& \times \sum_{k=0}^{\infty} d_k \left(\frac{\tau}{4}\right)^{-\left(\frac{\alpha+k}{2}\right)} \gamma\left(\frac{\alpha+k}{2}, \frac{\tau}{4}\left(\frac{\rho}{1+\rho}\right)^2\right) \\
& + \alpha(1+\rho)\left(1+\frac{1}{\rho}\right)^{\frac{\alpha-1}{2}} I_{\alpha-1}\left(2\sqrt{\alpha\rho}\right) \\
& \times \sum_{k=0}^{\alpha-2} e_k \left(\frac{\tau}{4}\right)^{-\left(\frac{k+1}{2}\right)} \Gamma\left(\frac{k+1}{2}, \frac{\tau}{4}\left(\frac{\rho}{1+\rho}\right)^2\right) \qquad (16) \\
& + \left[\alpha(1+\rho)\right]^{\beta/2}\left(1+\frac{1}{\rho}\right)^{\frac{\alpha-1}{2}} I_{\alpha-1}\left(2\sqrt{\alpha\rho}\right) \\
& \times \sum_{k=0}^{\infty} f_k \left(\frac{\tau}{4}\right)^{-\left(\frac{2\alpha+2k+1}{4}\right)} \Gamma\left(\frac{2\alpha+2k+1}{4}, \frac{\tau}{4}\left(\frac{\rho}{1+\rho}\right)^2\right) \\
& + \alpha(1+\rho)\left(1+\frac{1}{\rho}\right)^{\frac{\alpha-1}{2}} I_{\alpha-1}\left(2\sqrt{\alpha\rho}\right) \\
& \times \sum_{k=0}^{\infty} \left(g_k - f_k\right) \left(\frac{\tau}{4}\right)^{-\left(\frac{\alpha+k}{2}\right)} \Gamma\left(\frac{\alpha+k}{2}, \frac{\tau}{4}\left(\frac{\rho}{1+\rho}\right)^2\right)\Bigg]^{|\Omega|}
\end{aligned}
$$

IV. Numerical Results

In this section, we will first compare the derived approximate bounds with exact Chernoff bounds. Then, as an example, we will consider a convolutionally coded system and will use our bounds on PEP to compute upper bounds on the bit error rate (BER) performance of the considered system.

We first focus on the *K* channel, investigating the accuracy of derived bound on PEP given by (12). In Fig. 1, we present (12) for different truncation values, (i.e. $k = 0,1,...,t$ and $t = 1,2,3,4$) and for different α values. We also compute the exact Chernoff bound given by (8) using numerical integration and provide it as a reference (illustrated by dashed lines). It is seen that for $\alpha = 2$ truncation effect is observed easily, where an increase in *t* results in the improvement of the bound. We also observe that increasing *t* larger than 4 (not shown in the figure) does not result in a further improvement. The approximate and Chernoff bounds coincide as SNR goes higher. For $\alpha = 4$, similar observations hold and derived bound coincides with the exact Chernoff bound even in the lower SNR region. For $\alpha = 40$, even a truncation length of $t = 1$ yields a perfect match to the exact bound within the considered SNR range. Note that corresponding exact bound for this case is not observable in the figure because of perfect overlapping. In the Fig.1, we also include the bound given by (7) for the negative exponential channel. The bound for $\alpha = 40$ stands very close to that for the negative exponential distribution as expected since the *K* distribution reduces to the negative exponential for the limiting case of $\alpha \to \infty$.

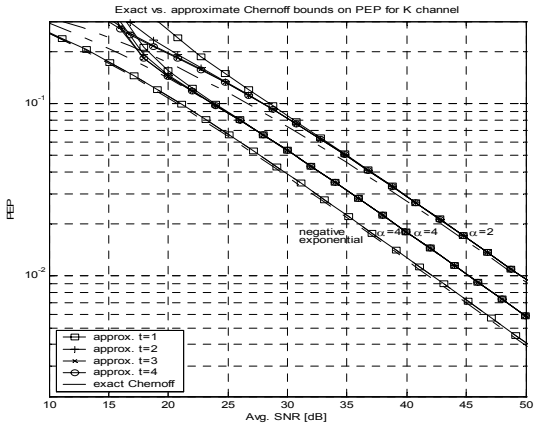

Fig. 1. Exact vs. approximate Chernoff bounds on PEP for the *K* channel (α=2, 4, 40)

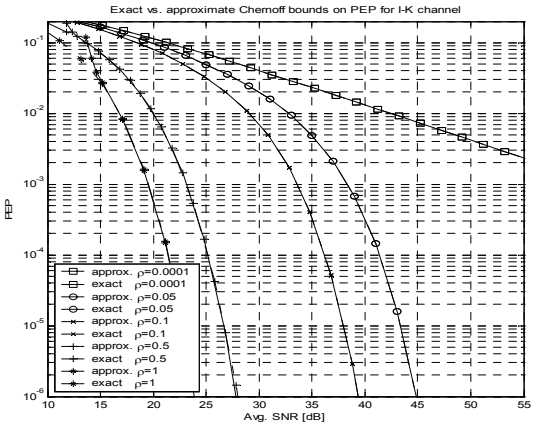

Fig. 2. Exact vs. approximate bounds on PEP for the *I-K* channel (α=20)

In Fig. 2, derived bounds for the *I-K* channel given by (16) are illustrated for $\alpha = 20$ with various values of the coherence parameter, ρ. In all computations, only four terms are kept in the first summation, truncating the infinite summation. The third and fourth summations (which essentially correspond to similar expressions for the *K* channel) are truncated to five terms (i.e. $t = 4$). The exact Chernoff bounds for the corresponding ρ values are computed by the numerical integration of (13) and are included in the figure as dashed lines. The comparison of bounds shows that approximate bounds yield very good match to the exact ones. Especially for the larger values of ρ, they yield identical results (Due to perfect overlapping, the dashed lines are not observable in the figure for these cases). The illustrations for various values of ρ allow us also to investigate the behavior of the *I-K* channel under different turbulence conditions. For small values of the coherence parameter, the *I-K* channel behaves in a similar manner to the *K* channel. In our numerical results, we ac-

tually find a perfect match between the performance of the *K* channel and that of the *I-K* channel with $\rho = 10^{-4}$. As the coherence parameter increases, turbulence effect decreases leading to weak turbulence regime and the system performance improves significantly.

In the following we consider the BER performance. A union bound on the average BER of a convolutionally coded system is given as [11]

$$P_b \le \frac{1}{n}\frac{\partial}{\partial s} T(D,s)\Big|_{s=1}$$

where $T(D,s)$ is the transfer function associated with the error state diagram of the convolutional code, *s* is an indicator variable and *D* parameter is defined based on the PEP expression for the channel model under consideration.

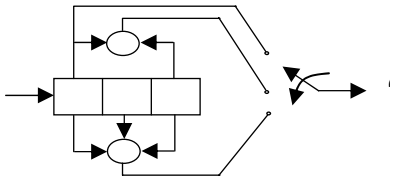

Fig. 3. Rate=1/3 convolutional encoder with constraint length 3 [11].

As an example, we consider the convolutional code in Fig.3 [11], which has a code rate of 1/3 and constraint length of 3. The average BER results are computed based on the transfer function technique and illustrated in the Fig. 4 and Fig. 5 for the *K* and *I-K* channels, respectively. In Fig. 4, analytical results for the *K* channel with $\alpha = 10$ and $\alpha = 40$ are given along with the corresponding simulation results. Performance for the negative exponential channel is also included. Similar to PEP results, the *K* channel with $\alpha = 40$ has a very similar performance to that over the negative exponential channel as expected. Simulation results also agree well with analytical bounds, demonstrating the accuracy of derived approximate PEP expressions. In Fig. 5, analytical bounds for the *I-K* channel with $\alpha = 20$ for various ρ values are illustrated. Simulation results are again included and seem to be in good agreement with analytical results as for the *K* channel.

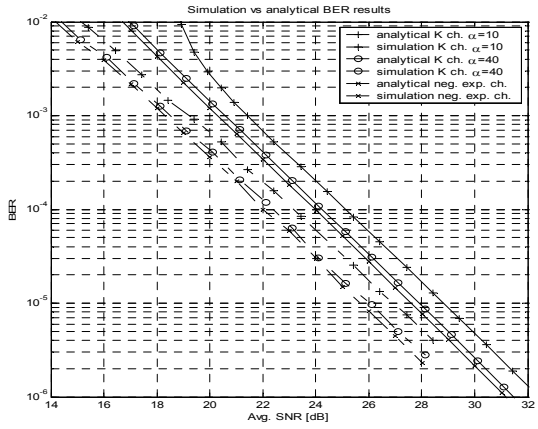

Fig. 4. Upper bounds on the BER for the *K* channel. (solid: upper bound, dashed: simulation)

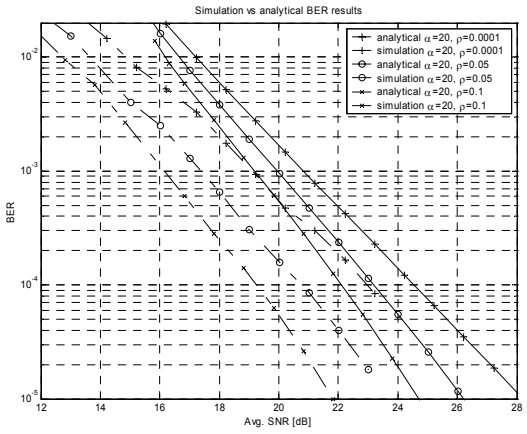

Fig. 5. Upper bounds on the BER for the *I-K* channel (solid: upper bound, dashed: simulation)

V. CONCLUSIONS

In this paper, we derived error performance bounds for coded wireless optical links operating over atmospheric channels. The analysis was carried out for three different atmospheric channel models, where the turbulence-induced fading was modeled by the negative exponential distribution, *K* distribution and *I-K* distribution. We derived bounds on the pairwise error probability for each distribution and then applied the transfer function technique in conjunction with derived bounds to obtain upper bounds on the bit error rate performance. Simulation results were also included to confirm the analytical results.

REFERENCES

[1] H. Willebrand and B. S. Ghuman, *Free Space Optics: Enabling Optical Connectivity in Today's Networks*, Sams Publishing, 2002.

[2] L. Andrews, R. L. Phillips and C. Y. Hopen, *Laser Beam Scintillation with Applications*, SPIE Press, 2001.

[3] J. Li and M. Uysal, "Achievable Information Rate for Outdoor Free Space Optical Communication with Intensity Modulation and Direct Detection", accepted for presentation at *IEEE GLOBECOM'03*, San Francisco, California, USA, December 2003.

[4] X. Zhu and J. M. Kahn, "Performance Bounds for Coded Free-Space Optical Communications through Atmospheric Turbulence Channels", *IEEE Trans. on Commun.*, vol. 51, no. 8, pp. 1233-1239, August 2003.

[5] E. Jakeman and P. N. Pusey, "A model for non-Rayleigh sea echo", *IEEE Transactions on Antennas and Propagation*, vol. 24, no. 6, pp.806-814, November 1976.

[6] E. Jakeman and P. N. Pusey, "The significance of K-distributions in scattering experiments", *Physical Review Letters*, vol. 40, no. 9, p. 546-550, February 1978.

[7] E. Jakeman, "On the statistics of K-distributed noise", *Journal of Physics A*, vol.13, p. 31-48, 1980.

[8] L. C. Andrews and R. L. Phillips, "I-K distribution as a universal propagation model of laser beams in atmospheric turbulence", *Journal of Optical Society of America A*, vol. 2, no. 2, P. 160-163, February 1985.

[9] L. C. Andrews and R. L. Phillips, "Mathematical genesis of the I-K distribution for random optical fields", *Journal of Optical Society of America A*, vol. 3, no. 11, p. 1912-1919, November 1986.

[10] I. S. Gradshteyn and I. M. Ryzhik, *Table of Integrals, Series and Products*, Academic Press, 1994.

[11] J. G. Proakis, *Digital Communications*, McGraw-Hill, 3rd ed., 1995.